View metadata, citation and similar papers at core.ac.uk

brought to you by CORE

provided by UCL Discovery

Nonlinear Analysis: Real World Applications 41 (2018) 570–587

Contents lists available at ScienceDirect

Nonlinear Analysis: Real World Applications

www.elsevier.com/locate/nonrwa

Nonmonotone invariant manifolds in the Nagylaki–Crow model☆

Belgin Seymenoglu*, Stephen Baigent

Department of Mathematics, University College London, Gower Street, London WC1E 6BT, United Kingdom

ARTICLE INFO

Article history:
Received 16 June 2017
Received in revised form 19 November 2017
Accepted 21 November 2017
Available online 14 December 2017

Keywords:
Invariant manifolds
Population genetics
Nagylaki–Crow model

ABSTRACT

We use a change of dynamical variables to prove, subject to certain conditions on the parameters, that a nonmonotone invariant manifold exists and is the graph of a convex function for the planar Nagylaki–Crow fertility–mortality model from population genetics with $n = 2$. Our results are obtained without the common assumption that fertilities or death rates are additive, and are not restricted to the case that the model is competitive in the new coordinates. We also provide numerical examples demonstrating that the manifold need not be the graph of a convex function, smooth, unique or globally attracting, and that the model exhibits a sequence of nonmonotone manifolds similar to those studied by Hirsch for competitive Kolmogorov systems (Hirsch 1988).

© 2017 The Author(s). Published by Elsevier Ltd. This is an open access article under the CC BY license (http://creativecommons.org/licenses/by/4.0/).

1. Introduction

In this paper we study invariant manifolds for the Nagylaki–Crow model, a continuous-time model from population genetics, sometimes referred to as the fertility–mortality model [1], because these are the two opposing forces at play for the model. By fertility, we mean the average number of offspring produced per unit time by parents with specified genotypes. Meanwhile, mortality refers to the death rate for a given (parental) genotype.

One of the earliest attempts at considering different fertilities for mating pairs was made by Penrose in [2]. He showed that his basic discrete-time model with additive fertilities gave essentially the same results as the usual discrete selection model. For the next few decades, most investigations into differential fertility were only made for the discrete model [3].

Then in 1961 Rucknagel and Neel produced experimental evidence of fertility differences among mating pairs for the locus corresponding to sickle cell anaemia [4], a single-locus genetic disorder affecting humans. This revived interest in differential fertility models.

☆ Supported by the EPSRC (no. EP/M506448/1) and the Department of Mathematics, UCL.

* Corresponding author.
E-mail addresses: belgin.seymenoglu.10@ucl.ac.uk (B. Seymenoglu), steve.baigent@ucl.ac.uk (S. Baigent).

https://doi.org/10.1016/j.nonrwa.2017.11.011
1468-1218/© 2017 The Author(s). Published by Elsevier Ltd. This is an open access article under the CC BY license (http://creativecommons.org/licenses/by/4.0/).

Over a decade later, Nagylaki and Crow provided a derivation for a continuous-time model [5,6], now known as the Nagylaki–Crow model. However, they restricted their attention to the case of additive fertilities when analysing the model. Another special case of this model is analysed in [7,8] with symmetric fertilities and no deaths. Hadeler and Glas showed that all orbits for the Nagylaki–Crow model with no deaths converge to some fixed point [9]. They also proposed a change of variables, which was later used in [10] to demonstrate that the model can have periodic orbits. In the nineties, Szucs proved the existence of an invariant manifold connecting the two heterozygotic fixation states in a two allele fertility-selection model where the fertilities were additive. He also showed that with the assumption of additivity of mortalities [11] this invariant manifold coincided with the Hardy–Weinberg manifold where the genotypic frequencies are the product of allele frequencies. Szucs and Akin also showed in [12] that with additivity of positive fertilities and mortalities the Hardy–Weinberg manifold is invariant, and with additional conditions on the relative sizes of fertilities and differences in mortalities implied convergence of solutions onto the Hardy–Weinberg manifold.

Our aim here is to extend this work by showing that the Nagylaki–Crow model possesses at least one nonmonotone invariant manifold *without assuming additivity of fertilities or mortalities*, which will make our result more widely applicable than Akin and Szucs. In the context of our planar model, a nonmonotone manifold is a manifold which is the graph of a decreasing continuous function; the full definition for a manifold being nonmonotone is given later in Section 3. We also find conditions that ensure that the invariant manifold is the graph of a convex function, as is the case for the Hardy–Weinberg manifold.

Section 2 introduces the n-allele model, while Section 3 discusses the two-allele case of the model and shows how to rewrite the Nagylaki–Crow model as a competitive system using a change of coordinates, although later we will drop one of the two inequalities that render the model competitive, so that we obtain results for not-necessarily competitive models. It turns out that the model always has fixed points on two corners of the triangular phase plane (axial fixed points) corresponding to heterozygotic fixation, and our numerical evidence suggests the existence of at least one nonmonotone invariant manifold Σ connecting the two fixed points in the phase plot. We analyse both axial fixed points in Section 4, and investigate their relationship with the condition for the system being competitive in the new coordinates. Finally, for Section 5, we prove that a nonmonotone invariant manifold Σ does indeed exist for a certain case of the Nagylaki–Crow model, and that it is the graph of a convex function. When the fertilities and mortalities are additive, Σ coincides with the Hardy–Weinberg manifold.

2. The model

A derivation of the panmictic Nagylaki–Crow model for diploid populations can be found in [5], where the authors consider a single locus with n alleles $A_1, \ldots, A_n$, and the dynamical variables of their system are the frequencies P_{ij} for the ordered genotype A_iA_j.

The Nagylaki–Crow model also features the fertilities $a_{ik,lj}$ that are defined as the product of the average number of matings of an arbitrary individual per unit time and the average number of progeny per $A_iA_k \times A_lA_j$ union. With this definition in mind, it is reasonable to assume

$$a_{ik,lj} \geq 0 \quad \forall i, j, k, l.$$

Moreover, it will be assumed that these fertilities are also time-independent for all i, j, k, l.

In addition, the model contains the mortalities d_{ij}, the death rate for genotype A_iA_j. These are also taken to be non-negative and constant for all time.

The governing equations for the genotype frequencies P_{ij}

$$\dot{P_{ij}} = \left(\sum_{kl} a_{ik,lj} P_{ik} P_{lj} - d_{ij} P_{ij} \right) - P_{ij} \sum_{uv} \left(\sum_{kl} a_{uk,lv} P_{uk} P_{lv} - d_{uv} P_{uv} \right), \tag{2.1}$$

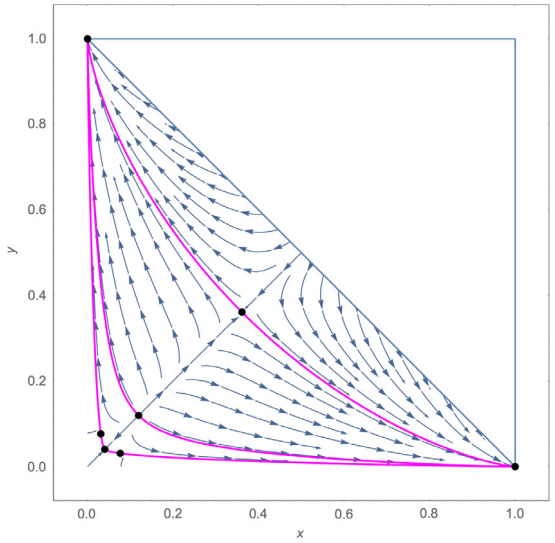

Fig. 1. A case of the Nagylaki–Crow model with five interior fixed points, three of which occur on the line $y = x$ with $y = 0.04, 0.12$ and 0.36 respectively. There are three different nonmonotone invariant manifolds, one of which passes through three interior fixed points. Here, the fertilities are $F_{11} = 6$, $F_{12} = 1/2$, $F_{13} = 1$, $F_{22} = 1/14$, $F_{23} = 1/2$, $F_{33} = 6$, while the mortalities are $D_1 = 2$, $D_2 = 1$, $D_3 = 2$, making this system competitive in (w, t) coordinates. The notation for the fertilities and mortalities are as given in (3.2) and (3.3).

form a system of n^2 nonlinear first order ordinary differential equations (see [5] or [6]). Note that if $P_{ij}(0) \geq 0$ then $P_{ij}(t) \geq 0$ for all $t \geq 0$. Moreover $\sum_{i,j=1}^{n} P_{ij}(t) = 1$ for all $t \geq 0$. The marginal $\sum_{j=1}^{n} P_{ij}(t) = \sum_{j=1}^{n} P_{ji}(t) = p_i(t)$ is the frequency of allele A_i at time $t \geq 0$.

Fig. 1 shows an example of the phase portrait for the Nagylaki–Crow model. In this example, there are five interior fixed points, which is the maximum number that the two-allele model can possess [1]. In the figure there are three different nonmonotone invariant manifolds, one of which passes through three interior fixed points.

Even for this simple model it is not possible to obtain self-contained evolution equations for the allele frequencies, which often are the variables of most interest to the geneticist. However, the presence of an attracting manifold means that differential equations can be obtained for the allele frequencies when restricted to that manifold. If an initial point is attracted to the manifold rapidly then after a short transient the equations for the allele frequencies on the manifold will be a good approximation of the true allele frequencies. Note that if there is more than one attracting manifold, which manifold is approached will depend upon the initial conditions.

The special case where the fertilities and mortalities are additive means that $a_{ik,lj} = \alpha_{ik} + \beta_{lj}$ and $d_{ij} = \mu_i + \kappa_j$, where $\alpha_{ik}, \beta_{lj}, \mu_i, \kappa_j \geq 0$. In this special case all trajectories converge to this nonmonotone invariant manifold connecting the axial fixed points [12]. The Hardy–Weinberg manifold is obtained by solving $P_{11} = x^2$, so that it is the graph of the strictly convex function $\varphi_{HW} : [0, 1] \to [0, 1]$ defined by

$$\varphi_{HW}(x) = 1 + x - 2\sqrt{x}. \tag{2.2}$$

For comparison, the Hardy–Weinberg manifold is shown in Fig. 2. Our results show that under mild conditions, when the condition of additivity of fertilities and mortalities is relaxed, there is at least one such nonmonotone manifold, and we give conditions that ensure that any such nonmonotone manifold is the graph of a convex function. A detailed analysis of concerning uniqueness or nonuniqueness of this manifold will be discussed elsewhere.

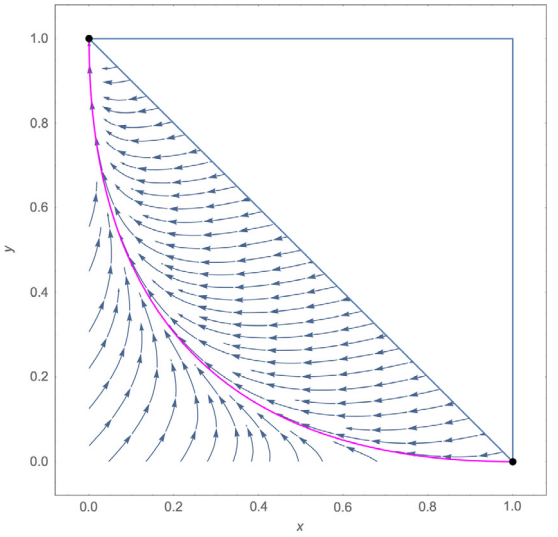

Fig. 2. An example where the fertilities are additive, leading to the Hardy–Weinberg manifold which is the graph of the function φ_{HW} in Eq. (2.2). Here, the fertilities are $F_{11} = 0.6$, $F_{12} = 0.9$, $F_{13} = 1.3$, $F_{22} = 1.2$, $F_{23} = 1.6$, $F_{33} = 1.3$, while the mortalities are $D_1 = 0.3$, $D_2 = 0.25$, $D_3 = 0.2$, making this system competitive in (w, t) coordinates. Again, the notation for the fertilities and mortalities are as given in (3.2) and (3.3).

3. Rewriting the Nagylaki–Crow model

Even for $n = 2$ the Nagylaki–Crow is not a straightforward model to analyse and to the best of the authors' knowledge there is currently no understanding of this model for three or more alleles [1].

In the sequel we will always assume $n = 2$ and ignore the order of the genotypes, i.e. treat the genotypes A_iA_j and A_jA_i as identical.

It is assumed in [6], as is done here, that the fertilities $a_{ik,lj}$ possess the symmetries

$$a_{ij,kl} = a_{kl,ij} = a_{ji,kl}. \tag{3.1}$$

Thus the Nagylaki–Crow model has only six independent fertility parameters. Using the notation of [10] these are relabelled as follows:

$$\begin{aligned} F_{11} &= a_{11,11}, \quad & F_{33} &= a_{22,22}, \\ F_{12} &= a_{11,12}, \quad & F_{23} &= a_{12,22}, \\ F_{22} &= a_{12,12}, \quad & F_{13} &= a_{22,11}. \end{aligned} \tag{3.2}$$

Meanwhile, as $d_{12} = d_{21}$, there are only three independent mortality parameters. They are rewritten as

$$D_1 = d_{11}, \quad D_2 = d_{12}, \quad D_3 = d_{22}. \tag{3.3}$$

Moreover, since the genotypes $A_iA_j = A_jA_i$, one has

$$P_{ij} = P_{ji}.$$

With this symmetry law in mind, let

$$P_{11} = x, \quad P_{12} = P_{21} = z/2, \quad P_{22} = y. \tag{3.4}$$

Then according to [10], the Nagylaki–Crow model (2.1) reduces to

$$\dot{x} = F_{11}x^2 + F_{12}xz + \frac{1}{4}F_{22}z^2 - D_1x - x\bar{m}, \tag{3.5}$$

$$\dot{z} = F_{12}xz + 2F_{13}xy + F_{23}yz + \frac{1}{2}F_{22}z^2 - D_2z - z\bar{m}, \tag{3.6}$$

$$\dot{y} = F_{33}y^2 + F_{23}yz + \frac{1}{4}F_{22}z^2 - D_3y - y\bar{m}, \tag{3.7}$$

with mean fitness

$$\begin{aligned}\bar{m} &= \sum_{uv}\left(\sum_{kl} a_{uk,lv}P_{uk}P_{lv} - d_{uv}P_{uv}\right)\\ &= F_{11}x^2 + 2F_{12}xz + F_{22}z^2 + 2F_{23}yz + 2F_{13}xy + F_{33}y^2\\ &\quad - D_1x - D_2z - D_3y.\end{aligned}$$

However, one also has the following condition:

$$\sum_{ij} P_{ij} = 1 \qquad \text{or} \qquad x + y + z = 1, \qquad x, y, z \geq 0 \tag{3.8}$$

which indicates that the two-allele Nagylaki–Crow model has in fact only two degrees of freedom and is fully described by just two ordinary differential equations on the phase space given by the triangle

$$T = \{(x, y) \in \mathbb{R}^2_+ : x + y \leq 1\}. \tag{3.9}$$

(Here and elsewhere $\mathbb{R}_+ = [0, \infty)$). These ordinary differential equations can be written in the form

$$\dot{x} = f(x, y), \qquad \dot{y} = g(x, y), \tag{3.10}$$

by substituting $z = 1 - x - y$ into the x and y equations. The full equations for x, y can be found in Appendix.

As an alternative, we use the following coordinate change introduced in [9,10]

$$(x, y) \mapsto (w, t) = \Phi(x, y) := \left(\frac{2x}{1 - x - y}, \frac{2y}{1 - x - y}\right). \tag{3.11}$$

The map Φ is a diffeomorphism from the interior of T to the interior of $\mathbb{R}^2_+$ with inverse

$$\Phi^{-1}(w, t) = \left(\frac{w}{2 + w + t}, \frac{t}{2 + w + t}\right) \tag{3.12}$$

and the Jacobian J of Φ on the interior of T is given by

$$J = \begin{pmatrix} -\dfrac{2(y-1)}{(x+y-1)^2} & \dfrac{2x}{(x+y-1)^2} \\ \dfrac{2y}{(x+y-1)^2} & -\dfrac{2(x-1)}{(x+y-1)^2} \end{pmatrix}, \quad \det J = \frac{4}{(1 - x - y)^3}. \tag{3.13}$$

In the new coordinates, the system (3.10) reduces to

$$\dot{w} = p(w, t), \qquad \dot{t} = q(w, t), \tag{3.14}$$

where

$$\begin{aligned} p(w, t) &= (F_{11} - F_{12} + D_2 - D_1)w^2 + (2(F_{12} + D_2 - D_1) - F_{22})w\\ &\quad + F_{22} - wt(F_{23} - D_2 + D_1 + F_{13}w), \end{aligned} \tag{3.15}$$

$$\begin{aligned} q(w, t) &= (F_{33} - F_{23} + D_2 - D_3)t^2 + (2(F_{23} + D_2 - D_3) - F_{22})t\\ &\quad + F_{22} - wt(F_{12} - D_2 + D_3 + F_{13}t). \end{aligned} \tag{3.16}$$

Here by $\dot{w}, \dot{t}$ we mean differentiation with respect to time; time will be denoted by s in the sequel.

In this set of coordinates, the phase space is the whole (non-compact) first quadrant $w \geq 0, t \geq 0$. For the boundary $w = 0$, one has $\dot{w} = F_{22} \geq 0$, which shows that $w < 0$ can never occur. Likewise, we have $\dot{t} = F_{22} \geq 0$ for the boundary at $t = 0$, therefore it is impossible to acquire $t < 0$. This indicates that the phase space $\mathbb{R}^2_+$ is forward invariant.

The off-diagonal elements of the Jacobian for this system are

$$p_t = (-F_{23} + D_2 - D_1)w - F_{13}w^2$$
$$q_w = (-F_{12} + D_2 - D_3)\,t - F_{13}t^2,$$

which are both non-positive for all $w, t \geq 0$ if and only if

$$D_2 \leq \min(D_1 + F_{23}, D_3 + F_{12}). \tag{3.17}$$

Inequality (3.17) is a necessary and sufficient condition for Eqs. (3.14) to be competitive on $\mathbb{R}^2_+ = \{(w,t) \in \mathbb{R}^2 : w \geq 0, t \geq 0\}$, i.e. $p_t, q_w \leq 0$ [9,10]. It is known that an orbit of a planar competitive system is either unbounded or converges to a fixed point in increasing time [1,9]. For this system, if an orbit Γ in (w,t) is unbounded, then $z \to 0$, i.e. $(x + y) \to 1$. This shows that the corresponding ω-limit set for Γ in (x,y) coordinates is a subset of the bounding line $x + y = 1$.

As shown by Hirsch [13] competitive systems often possess special codimension-1 invariant manifolds Σ that are nonmonotone, so that no two points on Σ may be ordered with respect to the partial order that defines the competitive ordering. Here we use the standard first orthant ordering: For each $i = 1, 2$, $x \geq y$ if and only if $x_i \geq y_i$; $x > y$ if and only if $x \geq y$ and $x \neq y$, $x \gg y$ if and only if $x_i > y_i$. A manifold Σ is said to be nonmonotone if no points $x, y \in \Sigma$ satisfy $x < y$; this agrees with our definition above that Σ is the graph of a decreasing continuous function. Examples of nonmonotone manifolds are the three solid curves in Fig. 1. Hirsch [13] showed that a large class of competitive ordinary differential equations possess a countable sequence of nonmonotone manifolds that divide the phase space into regions, and that these manifolds are alternately repelling and attracting. Although our model is competitive, it does not satisfy the setting of Hirsch's theory since $\partial\mathbb{R}^2_+$ is not invariant. However, we have found numerical evidence of similar sequences of nonmonotone manifolds. For example, Fig. 1 shows three nonmonotone manifolds (solid curves) that all connect the axial fixed points. These are the only *nonmonotone* invariant manifolds in the figure. A monotone invariant manifold (where points are ordered) passes through 3 interior fixed points along the line $x = y$. Two of the nonmonotone manifolds pass through a single interior fixed point, and the third passes through 3 interior fixed points. The detailed structure of alternate repelling and attracting nonmonotone manifolds in our model will be studied elsewhere. The focus in this paper is to prove the existence of at least one nonmonotone invariant manifold and to establish conditions that the manifold is the graph of a convex function. It turns out that to do this it is much easier to carry out some calculations in the (w,t) coordinates where phase space is not compact, mapping back results to the system in (x,y) coordinates, and some calculations in (x,y) coordinates where the phase space is compact, but there is no obvious ordering in (x,y) coordinates for which the system is monotone or competitive. Our key observation is that manifolds that are nonmonotone and graphs of convex functions in (w,t) coordinates are also nonmonotone and graphs of convex functions in (x,y) coordinates.

The first step is to prove the following lemma:

Lemma 3.1. *Suppose $\Gamma \subset \mathbb{R}^2_+$ is the graph of a twice-continuously differentiable function $\psi : (a,b) \subset \mathbb{R}_+ \to \mathbb{R}_+$ $(0 < a < b)$ such that*

$$\psi'(w) < 0, \quad \psi''(w) > 0, \ \forall w \in (a,b).$$

Then $\Gamma' = \Phi^{-1} \circ \Gamma$ *is the graph of a twice-continuously differentiable convex and decreasing function* $\phi : (A, B) \to \mathbb{R}_+$ *where* $A = \frac{a}{2+a+\psi(a)}, B = \frac{b}{2+b+\psi(b)}$, *and* $\psi = \phi \circ \Phi$*:*

$$\phi'(x) < 0, \quad \phi''(x) > 0, \ \forall x \in (A, B).$$

Proof. This is a simple calculation using that $(w, \psi(w)) = \Phi(x, \phi(x))$

$$\phi'(x) = \frac{(2+w)\psi'(w) - \psi(w)}{(2+\psi(w)) - w\psi'(w)}.$$

However, recall that $w, t = \psi(w) > 0$, therefore

$$\psi'(w) < 0 \quad \Rightarrow \quad \phi'(x) < 0. \tag{3.18}$$

Furthermore,

$$\phi''(x) = \frac{2(2+w+\psi(w))^3}{(2+\psi(w) - w\psi'(w))^3}\, \psi''(w). \tag{3.19}$$

Again, using $w, t = \psi(w) > 0$ we deduce

$$\psi'(w) < 0, \quad \psi''(w) > 0 \quad \Rightarrow \quad \phi''(x) > 0. \quad \square \tag{3.20}$$

Remark. It is known that linear-fractional transformations such as Φ map convex sets to convex sets (see, for example, [14]). Hence graphs of convex functions in (w, t) coordinates map to graphs of convex functions in (x, y) coordinates.

Regarding interior fixed points,

Lemma 3.2. *A fixed point in the interior of* T *in* (x, y) *coordinates corresponds to a fixed point in the interior of* $\mathbb{R}^2_+$ *in* (w, t) *coordinates.*

Proof. Since $(w, t) = \Phi(x, y)$ we have $(\dot{w}, \dot{t}) = J(\dot{x}, \dot{y})$, where J is given by (3.13). Since J is invertible when $0 < x + y < 1$, and Φ maps the interior of T to the interior of $\mathbb{R}^2_+$, fixed points in $0 < x + y < 1$ correspond to interior fixed points in $\mathbb{R}^2_+$. $\square$

4. Fixed points and stability

The two fixed points $(1, 0)$ and $(0, 1)$ in T represent the cases where all members of the population are homozygotes A_1A_1 and A_2A_2 respectively. These two points are always fixed points for the model (3.10) regardless of the values of the parameters, and their local invariant manifolds are investigated via spectral analysis of the Jacobian

$$\mathbf{J} = \begin{pmatrix} f_x & f_y \\ g_x & g_y \end{pmatrix}$$

for both points.

One finds that the Jacobian corresponding to $(0, 1)$ is

$$\mathbf{J^{(0,1)}} = \begin{pmatrix} D_3 - D_1 - F_{33} & 0 \\ D_1 - D_2 - 2F_{13} + F_{23} & D_3 - D_2 + F_{23} - F_{33} \end{pmatrix},$$

with eigenvalues $\lambda_1^{(0,1)} = D_3 - D_1 - F_{33}$, $\lambda_2^{(0,1)} = D_3 - D_2 + F_{23} - F_{33}$.

For simplicity, we only consider the generic case where $(0,1)$ is a hyperbolic fixed point and $\lambda_1^{(0,1)} \neq \lambda_2^{(0,1)}$. If $D_1 - D_2 - 2F_{13} + F_{23} \neq 0$, suitable respective eigenvectors for $\lambda_1^{(0,1)}, \lambda_2^{(0,1)}$ are

$$\mathbf{v_1^{(0,1)}} = \left(-\frac{D_1 - D_2 + F_{23}}{D_1 - D_2 - 2F_{13} + F_{23}}, 1 \right)^T, \quad \mathbf{v_2^{(0,1)}} = (0,1)^T, \tag{4.1}$$

which indicates that the tangent space for one of the local invariant manifolds at $(0,1)$ is then vertical. The positioning relative to T of the local invariant manifold tangent to $\mathbf{v_1^{(0,1)}}$ is not immediately obvious. On closer inspection, it turns out that the local invariant manifold will lie locally in the triangular region T if and only if the gradient of its tangent line, spanned by, $\mathbf{v_1^{(0,1)}}$, is strictly less than -1, which occurs when $F_{23} < D_2 - D_1$. Notice that this condition is satisfied if and only if $\lambda_2^{(0,1)} < \lambda_1^{(0,1)}$. In the case that $D_1 - D_2 + F_{23} - 2F_{13} = 0$, so that $\mathbf{J^{(0,1)}}$ is diagonal, and since we are assuming that $\lambda_1^{(0,1)} \neq \lambda_2^{(0,1)}$, not a multiple of the identity, then $(1,0)$ and $(0,1)$ are suitable respective eigenvectors, and only $(0,1)$ lies in T. Note that for general F_{ij} and D_k the signs of the eigenvalues remain unspecified, hence it is unclear whether each local manifold is stable, unstable or centre.

Meanwhile, the Jacobian at $(1,0)$ is

$$\mathbf{J^{(1,0)}} = \begin{pmatrix} D_1 - D_2 + F_{12} - F_{11} & D_3 - D_2 + F_{12} - 2F_{13} \\ 0 & D_1 - D_3 - F_{11} \end{pmatrix},$$

which has eigenvalues

$$\lambda_1^{(1,0)} = D_1 - D_3 - F_{11}, \quad \lambda_2^{(1,0)} = D_1 - D_2 + F_{12} - F_{11}. \tag{4.2}$$

Similarly to above we assume that $(1,0)$ is hyperbolic and $\lambda_1^{(1,0)} \neq \lambda_2^{(1,0)}$.

When $D_3 - D_2 + F_{12} - 2F_{13} \neq 0$, $\mathbf{J^{(1,0)}}$ has suitable respective eigenvectors for $\lambda_1^{(0,1)}, \lambda_2^{(0,1)}$ given by

$$\mathbf{v_1^{(1,0)}} = \left(-\frac{D_3 - D_2 + F_{12} - 2F_{13}}{D_3 - D_2 + F_{12}}, 1 \right)^T, \quad \mathbf{v_2^{(1,0)}} = (1,0)^T.$$

Hence the tangent space for one local manifold at the point is guaranteed to be horizontal at $(1,0)$. A necessary condition for the respective tangent space of the other local invariant manifold being inside the triangle T is that the gradient of $\mathbf{v_1^{(1,0)}}$ should be strictly bounded by the values -1 and 0, or equivalently,

$$\frac{F_{13}}{D_3 - D_2 + F_{12}} < 0.$$

This is satisfied if $F_{12} < (D_2 - D_3)$, which is equivalent to $\lambda_2^{(1,0)} < \lambda_1^{(1,0)}$. Again, the two eigenvalues can be generally either positive, negative or zero, hence the respective tangent spaces corresponding with the local invariant manifolds could be stable, unstable or centre manifolds.

Note that since all fertilities and death rates are taken to be real numbers, the triangular Jacobian for both fixed points must always have real eigenvalues. Therefore, when hyperbolic, these fixed points cannot have spirals or centres in their vicinity.

The system is strongly competitive in (w,t) coordinates if and only if strict inequality in (3.17) holds, which is equivalent to the following inequalities combined

$$\begin{aligned} F_{23} > (D_2 - D_1) \quad &\Leftrightarrow \quad \lambda_2^{(0,1)} > \lambda_1^{(0,1)}, \\ F_{12} > (D_2 - D_3) \quad &\Leftrightarrow \quad \lambda_2^{(1,0)} > \lambda_1^{(1,0)}. \end{aligned}$$

As noted above, however, this means that the tangent spaces of the local manifolds corresponding to the eigenvector $\mathbf{v_1}$ for both $(0,1)$ and $(1,0)$ lie outside the (x,y) phase space T. Thus strong competitiveness in the (w,t) phase space is equivalent to the local invariant manifolds at $(0,1)$ being always vertical at that fixed point, and similarly, any local manifolds at $(1,0)$ are always horizontal at that point.

All this is summarised by the following result:

Proposition 4.1. *The following are equivalent:*

1. *Both* $\lambda_2^{(0,1)} > \lambda_1^{(0,1)}$ *and* $\lambda_2^{(1,0)} > \lambda_1^{(1,0)}$ *hold.*
2. *The Nagylaki–Crow model is strongly competitive in* (w,t) *coordinates.*
3. *The tangent spaces of the local manifolds corresponding to* $\mathbf{v_1^{(0,1)}}$ *and* $\mathbf{v_1^{(1,0)}}$ *lie outside the* (x,y) *phase space* T*.*

5. Existence of a nonmonotone invariant manifold

The aim of this section is to prove that at least one nonmonotone invariant manifold Σ does indeed exist when

$$F_{12} > D_2 - D_3,$$

and that it is the graph of a convex function if in addition

$$F_{11} > D_1 - D_3 > -F_{33}.$$

Here the first inequality is similar to the condition (3.17) for competition, except that $D_2 \leq D_1 + F_{23}$ is not required and the inequalities are now strict.

We recall that the time variable is denoted by s, so as to avoid confusion with the vertical coordinate t from Section 3.

5.1. In the original (x,y) coordinates

In the style of [15], we consider the temporal evolution of a function $\varphi : [0,1] \times [0,\tau_0) \to \mathbb{R}_+$ satisfying $\varphi(x,0) = \varphi_0(x)$ and

$$\varphi(1,s) = 0, \qquad \varphi(0,s) = 1 \qquad \forall s \in [0,\tau_0). \tag{5.1}$$

Here $\tau_0 > 0$ is the maximal time of existence of φ as a solution of the first order partial differential equation

$$\frac{d\varphi}{ds} = \varphi_s + f\varphi_x = g, \tag{5.2}$$

where f and g are defined as in Eqs. (3.10), and $\varphi_s = \frac{\partial \varphi}{\partial s}$, subject to boundary and initial conditions explained below.

We let Σ_s be the graph of $\varphi(\cdot, s)$ for $s \in [0,\tau_0)$ (we will later show that $\tau_0 = +\infty$). The boundary conditions (5.1) force the endpoints of Σ_s to remain fixed for all time. We let

$$\varphi_0(x) = (1-x)(1-\varepsilon x), \quad \text{where} \quad 0 < \varepsilon \ll 1. \tag{5.3}$$

When $\epsilon = 0$, $\varphi_0(x) = 1 - x$ and the image of the graph of φ_0 under Φ is not defined. But by choosing $\epsilon > 0$ small the graph G_0 of φ_0 is close to $x + y = 1$ and is mapped by Φ to the graph of a continuous function $\psi_0 : \left(\frac{2}{\epsilon}, \infty\right) \to \mathbb{R}_+$ given by

$$\psi_0(w) = \frac{2(\epsilon w - 2 - w)}{2 - \epsilon w}. \tag{5.4}$$

The aim is to show that Σ_s converges (in the Hausdorff metric) to some manifold Σ as $s \to \infty$.

Using d/ds to denote the time derivative which follows trajectories in the phase plane, differentiating Eq. (5.2) gives Lemma 2.1 from [15], which is

$$\frac{d\varphi_x}{ds} = g_x + (g_y - f_x - f_y\varphi_x)\varphi_x. \tag{5.5}$$

It is possible to investigate the right and left-sided limits of φ_x as $x \to 0, 1$ respectively, i.e. $\varphi_x(0+, s)$ and $\varphi_x(1-, s)$. These can be evaluated by substituting the expressions for f_x, f_y, g_x and g_y for $(x, y) = (0, 1)$ into Eq. (5.5) to obtain the following ordinary differential equation for $\varphi_x(0, s)$:

$$\frac{d\varphi_x}{ds}(0, s) = (\lambda_2^{(0,1)} - \lambda_1^{(0,1)})(\varphi_x(0, s) + 1) - 2F_{13} \tag{5.6}$$

whose initial condition is

$$\varphi_x(0, 0) = -1 - \varepsilon < -1.$$

Although this equation is separable, we will not calculate the explicit solution for $\varphi_x(0, s)$, although we do note that since (5.6) is linear $\varphi_x(0, s)$ is bounded for all finite forward and backward time. If $F_{13} > 0$ one concludes that $\varphi_x(0, s) < -1$ for all $s \geq 0$, which follows from the fact that when $\varphi_x(0, s) = -1$,

$$\frac{d\varphi_x}{ds}(0, s) < 0.$$

Meanwhile, if $F_{13} = 0$ one observes that $\varphi(\cdot, s) = -1 - \varepsilon$ is the unique solution of (5.6) satisfying $\varphi(\cdot, 0) = -1 - \varepsilon$. Thus for all $F_{13} \geq 0$ we have

$$\varphi_x(0, s) < -1, \ \forall s \geq 0. \tag{5.7}$$

Now we repeat the procedure for $(x, y) = (1, 0)$. This time we obtain a differential equation for $\varphi_x(1, s)$:

$$\frac{d\varphi_x}{ds}(1, s) = -\varphi_x[(\lambda_2^{(1,0)} - \lambda_1^{(1,0)})(\varphi_x + 1) - 2F_{13}\varphi_x], \tag{5.8}$$

with

$$\varphi_x(1, 0) = -1 + \varepsilon \in (-1, 0).$$

Therefore if $F_{13} > 0$, then $\varphi_x(1, s) = -1$ leads to

$$\frac{d\varphi_x}{ds}(0, s) > 0,$$

while if $F_{13} = 0$, $\varphi_x(\cdot, s) = -1+\varepsilon$ is the unique solution of (5.8) satisfying $\varphi(\cdot, 0) = -1-\varepsilon$. Finally, regardless of whether F_{13} is positive or zero, there is another solution corresponding to the function constantly equal to zero. Therefore, as the solution is bounded, one can conclude that

$$-1 < \varphi_x(1, s) < 0, \ \forall s \geq 0. \tag{5.9}$$

Note, however, that there may be no lower bound for $\varphi_x(0, s)$.

To obtain information on $\varphi_x(x, s)$ for $x \in (0, 1)$ and $s \in [0, \tau_0)$ using (5.5) and Lemma 2.1 in [15] is not so easy due to the complicated form of $g_x = \frac{1}{2}F_{22}(x-1) + 2y^2(F_{12} - F_{22} + F_{23} - F_{13}) + y(D_1 - D_2 + \frac{5}{2}F_{22} - 2F_{12} - F_{23}) + 2xy(2F_{12} - F_{11} - F_{22})$, whose sign on T is not obvious.

Eq. (5.5) can be differentiated to obtain an equivalent version of Lemma 3.1 in [15]. This governs the evolution of the convexity of φ through the value of φ_{xx}. However, this approach will not be pursued in this paper, since we have found it too involved to track the sign of φ_{xx}. Since an approach in (x, y) coordinates does not easily lead to establishing that $\varphi_x < 0$, $\varphi_{xx} > 0$, we revert to (w, t) coordinates where establishing convexity is simpler via Lemma 3.1.

5.2. In the new (w,t) coordinates

5.2.1. The set-up

We seek to map the graph of φ in T to the graph of a new function ψ in $\mathbb{R}^2_+$. The function $\psi(\cdot,s)$ satisfies the first order quasilinear partial differential equation

$$\psi_s + p(w,\psi(w,s))\psi_w = q(w,\psi(w,s)) \tag{5.10}$$

for suitably defined $w \in \mathbb{R}_+$. For $s \in [0,\tau_0)$, $\psi(\cdot,s)$ is known to exist since it is obtained from $\varphi(\cdot,s) : [0,1] \to \mathbb{R}$ via

$$(w(x,s),\psi(w(x,s),s)) = \left(\frac{2x}{1-x-\varphi(x,s)}, \frac{2\varphi(x,s)}{1-x-\varphi(x,s)}\right),\ x \in (0,1), s \in [0,\tau_0). \tag{5.11}$$

Also needed is an initial condition $\psi(w,0) = \psi_0(w)$, where ψ_0 is a function to be determined from φ_0.

Unfortunately the straight line $y = 1-x$ does not have a well-defined counterpart in (w,t) coordinates, and so is an inappropriate choice for an initial data curve to map onto ψ_0. Instead, we construct ψ_0 by defining φ_0 as given in (5.3), and transforming that into (w,t) coordinates (see Fig. 3). By substituting $y = \varphi_0(x)$ and $z = 1-x-y$ in Eqs. (3.11), we obtain

$$w = \frac{2}{(1-x)\varepsilon}, \qquad t = \frac{2(1-x\varepsilon)}{x\varepsilon}, \qquad x \in (0,1).$$

Then by eliminating x and letting $t = \psi_0(w)$, where $\psi_0 : (\frac{2}{\epsilon},\infty) \to \mathbb{R}_+$ we obtain the hyperbola

$$\psi_0(w) = \frac{-2(2+w-w\varepsilon)}{2-w\varepsilon}.$$

The graph of $\psi_0(w)$ lies in the open first quadrant with vertical and horizontal asymptotes $w = 2/\varepsilon$ and $t = 2(1-\varepsilon)/\varepsilon$ respectively. In addition,

$$(\psi_0)_w = \frac{-4}{(w\varepsilon-2)^2} < 0 \qquad (\psi_0)_{ww} = \frac{8\varepsilon}{(w\varepsilon-2)^3} > 0. \tag{5.12}$$

5.2.2. Equivalent boundary conditions

Boundary conditions for the partial differential equation (5.10) are needed, and should be equivalent to the boundary conditions in (5.1). It turns out that the equivalent condition is that ψ must have a horizontal and vertical asymptote at all times, even if the positions of these asymptotes vary in time. For now, these asymptotes will be said to occur at t^* and w^* respectively (both functions of s).

Let us determine the boundary condition for (5.10) corresponding to the point $(0,1)$ using the transformation (3.11). Recall that $\varphi(\cdot,s) : [0,1] \to \mathbb{R}$ is defined and smooth for each $s \in [0,\tau_0)$. Then by l'Hôpital's rule, for all $s \in [0,\tau_0)$ we have $\lim_{x\to 0+} w(x,s) = \frac{2}{-1-\varphi_x(0,s)}$, whereas $\lim_{x\to 1-} w(x,s) = +\infty$. Similarly, $\lim_{x\to 0+} t(x,s) = +\infty$, whereas $\lim_{x\to 1-} t(x,s) = \frac{2\varphi_s(1,s)}{-1-\varphi_x(1,s)}$. The graph of $\psi(\cdot,s)$ has a vertical asymptote at $w = w^*(s) := \frac{2}{-1-m_0(s)}$ and a horizontal asymptote at $t = t^*(s) := \frac{2m_1(s)}{-1-m_1(s)}$, where $m_0(s) = \varphi_x(0,s)$ and $m_1(s) = \varphi_x(0,s)$. Since from (5.7) and (5.9) we have, $m_0 < -1$ and $-1 < m_1 < 0$, we find that $w^*(s), t^*(s)$ are well-defined and positive for $s \in [0,\tau_0)$. Hence the image of each $\varphi(\cdot,s)$ under Φ is a continuous curve that is the graph of a function $\psi(\cdot,s) : (w^*(s),+\infty) \to \mathbb{R}$. This indicates that both asymptotes will lie in the interior of $\mathbb{R}^2_+$.

5.2.3. Investigating the gradient and convexity

Differentiating Eq. (5.10) gives Lemma 2.1 from [15], which is

$$\frac{d\psi_w}{ds} = q_w + (q_t - p_w - p_t\psi_w)\psi_w, \quad s \in [0,\tau_0). \tag{5.13}$$

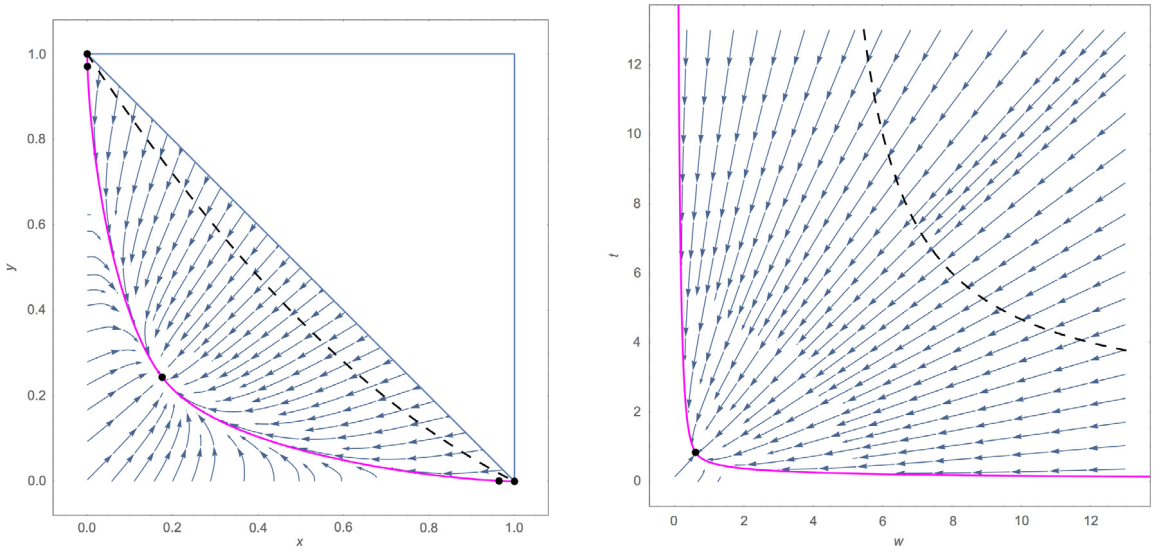

(a) A plot of the initial data curve, the graph of φ_0, in (x, y) coordinates.

(b) A plot of the initial data curve, the graph of ψ_0, in (w, t) coordinates.

Fig. 3. The initial data curve for the two coordinate systems (dashed line), which deforms in time according to the flow, converging to the invariant manifold Σ (solid line). For these plots, we take $\varepsilon = 1/2$.

Furthermore, we can repeat the procedure to obtain an equivalent version of Lemma 3.1 [15], which states that

$$\frac{d\psi_{ww}}{ds} = q_{ww} + \psi_w(2q_{wt} - p_{ww}) + \psi_w^2(q_{tt} - 2p_{wt}) - p_{tt}\psi_w^3 + \psi_{ww}(q_t - 2p_w - 3p_t\psi_w), \quad s \in [0, \tau_0). \tag{5.14}$$

However, as the equations of motion are already simpler in (w, t), the partial derivatives of p and q are also easier to compute. In fact, we find that

$$p_{tt} = q_{ww} = 0,$$

which simplifies Eq. (5.14) to

$$\frac{d\psi_{ww}}{ds} = \psi_w[(2q_{wt} - p_{ww}) + \psi_w(q_{tt} - 2p_{wt})] + \psi_{ww}(q_t - 2p_w - 3p_t\psi_w). \tag{5.15}$$

Also,

$$\begin{aligned} p_{ww} &= 2(D_2 - D_1 + F_{11} - F_{12} - F_{13}t), \\ q_{tt} &= 2(D_2 - D_3 + F_{33} - F_{23} - F_{13}w), \\ p_{wt} &= D_2 - D_1 - F_{23} - 2F_{13}w, \\ q_{wt} &= D_2 - D_3 - F_{12} - 2F_{13}t, \end{aligned}$$

and so

$$\begin{aligned} 2q_{wt} - p_{ww} &= 2(D_1 - D_3 - F_{11} - F_{13}t), \\ q_{tt} - 2p_{wt} &= 2(D_1 - D_3 + F_{33} + F_{13}w), \end{aligned}$$

which are negative and positive when $F_{11} > D_1 - D_3$ and $F_{33} > D_3 - D_1$ respectively. Combining these two conditions gives the constraint

$$F_{11} > D_1 - D_3 > -F_{33}, \tag{5.16}$$

which is equivalent to having both $\lambda_1^{(1,0)} < 0$ and $\lambda_1^{(0,1)} < 0$. Meanwhile, a sufficient condition for $q_w < 0$ is $t > 0$ and $D_2 < D_3 + F_{12}$ (i.e. $\lambda_2^{(1,0)} > \lambda_1^{(1,0)}$).

Then, assuming (5.16) and $D_2 < D_3 + F_{12}$, let $\alpha = \psi_w$ and $\beta = \psi_{ww}$ and rewrite Eqs. (5.13) and (5.15) as two coupled ordinary differential equations:

$$\frac{d\alpha}{ds} = A\alpha^2 + B\alpha + C \tag{5.17}$$

$$\frac{d\beta}{ds} = \alpha(D + E\alpha) + \beta(F + G\alpha), \tag{5.18}$$

where

$$A = -p_t \qquad E = q_{tt} - 2p_{wt} > 0$$
$$B = q_t - p_w \qquad F = q_t - 2p_w$$
$$C = q_w < 0 \qquad G = -3q_t$$
$$D = 2q_{wt} - p_{ww} < 0$$

are all continuous (in fact, polynomial) functions of w and ψ (which replaces t). We already found that ψ_0 is strictly decreasing and convex, with $\alpha_0 < 0$ and $\beta_0 > 0$, where $\alpha_0 = \alpha(w, 0)$ and $\beta_0 = \beta(w, 0)$. Now the aim is to prove

$$\alpha < 0, \qquad \beta > 0 \qquad \forall s \in [0, \tau_0), \tag{5.19}$$

for all values of w for which $\psi(w, s)$ is defined. In other words, if the initial data curve is both strictly decreasing and convex in (w, t) coordinates, then it will remain that way as s increases in $[0, \tau_0)$.

The following lemma is based on Corollary 2.2 of [15], whose proof makes use of the fact that $C = q_w < 0$:

Lemma 5.1. *If the smooth initial curve ψ_0 satisfies both $\psi_0 > 0$ and $(\psi_0)_w < 0$, then for all $s \in [0, \tau_0)$, $\psi(\cdot, s)$ is defined and smooth for all $w > w^*(s)$ (where $w^*(s)$ is the vertical asymptote of $\psi(\cdot, s)$ mentioned in the previous remark), with $\psi(\cdot, s) > 0$, $\psi_w(\cdot, s) < 0$ and $\psi_{ww}(\cdot, s) > 0$.*

Proof. We already know that $\varphi(\cdot, s) : [0, 1] \to \mathbb{R}$ exists for $s \in [0, \tau_0)$ for some $\tau_0 > 0$, and hence via the coordinate change Φ, $\psi(\cdot, s) : (w^*(s), \infty) \to \mathbb{R}$ satisfying (5.10) exists for all $s \in [0, \tau_0)$. The function $\psi(\cdot, s) : (w^*(s), \infty) \to \mathbb{R}$ also satisfies Eqs. (5.13) and (5.15) for $s \in [0, \tau_0)$.

As the vertical asymptote $w^*(s)$ is changing in time, it is convenient to rescale the asymptote to unity by a change of variables, taking

$$v = \frac{w}{w^*(s)}. \tag{5.20}$$

Note that $w^*(s) > 0$ for $s \in [0, \tau_0)$ so that this transformation is defined for at least $s \in [0, \tau_0)$.

We define $\tilde{\psi}(\cdot, s) : [1, \infty) \to \mathbb{R}_+$ via

$$\tilde{\psi}(v, s) = \psi(w, s) = \psi(v\, w^*(s), s), \quad s \in [0, \tau_0).$$

Now compute

$$\begin{pmatrix} \psi_w \\ \psi_s \end{pmatrix} = \begin{pmatrix} v_w & 0 \\ v_s & 1 \end{pmatrix} \begin{pmatrix} \tilde{\psi}_v \\ \tilde{\psi}_s \end{pmatrix},$$

so that via (5.20)

$$\begin{pmatrix} \psi_w \\ \psi_s \end{pmatrix} = \begin{pmatrix} \dfrac{1}{w^*(s)} & 0 \\ \dfrac{-ww^{*\prime}(s)}{(w^*(s))^2} & 1 \end{pmatrix} \begin{pmatrix} \tilde{\psi}_v \\ \tilde{\psi}_s \end{pmatrix}. \tag{5.21}$$

Next, using a similar argument to that used to obtain (5.13) and the Chain Rule, we have $\tilde{\psi}_v = w^*(s)\psi_w$ along with

$$\frac{d\tilde{\psi}_v}{ds} = w^* q_w + (q_t - p_w + (\ln w^*)' - \frac{p_t}{w^*}\tilde{\psi}_v)\tilde{\psi}_v, \quad v \geq 1, s \in [0, \tau_0), \tag{5.22}$$

and $(\tilde{\psi}_0)_v < 0$. Note that in Eq. (5.22) we find that

$$(\ln w^*)'(s) = -\frac{d\varphi_x(0,s)/ds}{1 + \varphi_x(0,s)},$$

which by (5.7) is bounded for $s \in [0, \tau_0)$.

Following Corollary 2.2 in [15], but with strict inequalities, we note that in (5.22) the term $w^* q_w < 0$ so that if $\tilde{\psi}_v = 0$ for some value of $v \geq 1$ and $s \in [0, \tau_0)$, then from (5.22) we have $\frac{d\tilde{\psi}_v}{ds} < 0$, and so we deduce that $\tilde{\psi}(v, s)$ is strictly decreasing for $v \geq 1$ and $s \in [0, \tau_0)$. In turn this implies from $\psi_w = \frac{d\tilde{\psi}_v}{ds}/w^*$ that

$$\alpha = \psi_w(w, s) < 0, \ \forall w > w^*(s), \ s \in [0, \tau_0). \tag{5.23}$$

Now we turn to the sign of $\beta = \psi_{ww}$. If we let $\theta = \alpha(D + E\alpha)$ and $\sigma = (F + G\alpha)$, (5.18) may be written as

$$\frac{d\beta}{ds} = \sigma\beta + \theta, \tag{5.24}$$

and $D < 0$, $E > 0$ which, combined with $\alpha < 0$, yields $\theta > 0$. But $\beta_0 > 0$, so by Lemma 4.1 from [15], $\beta > 0$ whenever $s \in [0, \tau_0)$. Thus (5.19) holds, which indicates that

$$\psi_{ww} > 0 \qquad \forall w > w^*(s), \forall s \in [0, \tau_0). \tag{5.25}$$

In particular, (5.25) together with (5.23) implies from Lemma 3.1 that

$$\varphi_x(x, s) < 0, \ \varphi_{xx}(x, s) > 0, \ \forall x \in (0, 1), \ s \in [0, \tau_0). \tag{5.26}$$

Now we show that we may take $\tau_0 = +\infty$.

Since $\varphi_{xx}(\cdot, s) > 0$, $\varphi_x(x, s)$ is increasing with $x \in (0, 1)$, and hence finite, for each $s \in [0, \tau_0)$. Let us suppose that $\varphi_x(\bar{x}, s_i)$ becomes unbounded as $i \to \infty$ for some sequence $s_i \to \tau_0$, and some $\bar{x} \in (0, 1)$. Since $\varphi_{xx}(x, s) > 0$ for $s \in [0, \tau_0)$ and $x \in (0, 1)$ we have that $\varphi_x(x, s) \leq \varphi_x(\bar{x}, s)$ for all $x \in [0, \bar{x}]$ and $s \in [0, \tau_0)$. In particular $\varphi_x(0, s) \leq \varphi_x(\bar{x}, s)$ for all $s \in [0, \tau_0)$ and so $\varphi_x(0, s_i) \leq \varphi_x(\bar{x}, s_i)$. Letting $i \to \infty$ shows that $\varphi_x(0, s_i)$ is unbounded below which contradicts that solutions to the ordinary differential equation (5.6) remain bounded in finite time. This contradiction shows that $\tau_0 = \infty$.

We have thus shown that $\varphi_x(0, s)$ exists and is finite for all $s \in \mathbb{R}_+$ and that $\varphi(0, s) = 1$, $\varphi(1, s) = 0$ for all $s \in [0, \tau_0)$, and hence $\varphi(\cdot, s) : [0, 1] \to \mathbb{R}$ is a strictly decreasing smooth convex function for all $s \geq 0$. □

By Lemma 2.7 from [15], the graph of each $\varphi(\cdot, s)$ is a nonmonotone Lipschitz manifold Σ_s with Lipschitz constant unity. By the Arzelà –Ascoli Theorem, the space of Lipschitz functions in a compact space is itself compact. Hence a sequence of Lipschitz manifolds, such as the one constructed from φ, will always have a convergent subsequence whose limit is in turn also a nonmonotone Lipschitz manifold which we call Σ. It is not immediate that Σ is invariant. However, as we now show, we do not need to select a subsequence as the sequence of manifolds Σ_s is actually monotone decreasing in $s \geq 0$, from which it follows that the limit Σ is invariant.

We rewrite (5.2) in the form

$$\varphi_s = \mathbf{N} \cdot \mathbf{f}, \tag{5.27}$$

where $\mathbf{f} = (f, g)$ and $\mathbf{N} = (-\varphi_x, 1)$ is the upward normal which normalises to $\mathbf{n}$.

As done in [15], we track the time evolution of $b = \mathbf{n} \cdot \mathbf{f}$, the component of the flow normal to the curve. Suppose that $\varphi_0(x) = 1 - x$. Then at $s = 0$, $\mathbf{n} = \frac{1}{\sqrt{2}}(1, 1)$ and

$$b = 2F_{13}x(x - 1),$$

which is negative for $x \in (0, 1)$, as long as $F_{13} > 0$. Moreover, if ε is sufficiently small, we still have the same sign for b at $s = 0$ for all $x \in (0, 1)$ when $\varphi_0(x) = (1 - x)(1 - \varepsilon x)$, since this initial data curve is a perturbation of $y = 1 - x$.

Next, we invoke Lemma 2.6 from [15], i.e.

$$\dot{b} = (\mathbf{n} \cdot \nabla\mathbf{f} \cdot \mathbf{n})\, b,$$

which shows that b, and in turn φ_s, stays negative for all $s > 0$. So the graphs Σ_s of $\varphi(\cdot, s)$ always move downwards with increasing s under the flow of the system for all positive time, hence the limiting manifold Σ is indeed invariant.

Hence we can summarise our results in the following theorem:

Theorem 5.2. *In the Nagylaki–Crow model (3.5)–(3.7) suppose that*

$$D_2 < D_3 + F_{12}, \quad F_{13} > 0. \tag{5.28}$$

Then the model has at least one nonmonotone invariant manifold that connects the fixed points $(0, 1)$ *and* $(1, 0)$ *in* $T = \{(x, y) \in \mathbb{R}^2_+ : 0 \le x + y \le 1\}$.

If in addition

$$F_{11} > D_1 - D_3 > -F_{33} \tag{5.29}$$

holds, this nonmonotone manifold is the graph of a convex function.

Observe that all of (3.17) is not needed, so existence works for not necessarily competitive models that satisfy (5.28) only. A similar result applies by interchanging w and t leading to a version of Theorem 5.2 with (5.28) replaced by $D_2 < D_1 + F_{23}$ and (5.29).

The nonmonotone invariant manifold of Theorem 5.2 is a connecting orbit that connects the two axial fixed points (possibly via other fixed points) in T. When both inequalities in (3.17) hold, so that the system is competitive, it is also monotone with the order $\geq_L$ defined by $x = (x_1, x_2) \geq_L y = (y_1, y_2)$ if and only if $x_1 \geq y_1$ and $x_2 \geq y_2$. In this case, existence of a connecting orbit (even with additional fixed points ordered by $\geq_L$) follows from [16]. Jiang [17] showed that for cooperative systems, this connecting orbit is unique if the Jacobian is irreducible at the two fixed points. Even if Jiang's result on irreducibility can be modified for planar competitive systems, in our model the Jacobian at the axial fixed points is reducible and so an alternative approach is needed to determine when the nonmonotone manifold is unique. In any case our existence result does not require a competitive model for existence, and so conditions for uniqueness of the manifold are not at all clear and will be dealt with elsewhere.

6. Discussion

We have shown the existence of a nonmonotone invariant manifold for a continuous-time differential fertility model in Population Genetics without requiring additivity of fertilities or mortalities, nor competitive dynamics.

To do this, we set up an invertible mapping between an evolving curve φ in (x, y) space and an evolving (unbounded) curve ψ in (w, t) space. Through our lemmata it then suffices to check the signs of the first and second derivatives of ψ (as it then follows that the graph of φ is decreasing and convex). Then convergence is established in (x, y) space using Lipschitz and bounded sequences of the graph of φ. Thus the crucial part is setting up the map between φ and ψ by a change of dynamical variables. A similar technique is remarked on in [18] which involves applying the transformation $y_i = \log x_i$ $(i = 1, 2, 3)$ on the Lotka–Volterra equations. This coordinate change maps the invariant surface from something which is not necessarily concave to a concave surface.

There was no need to assume that the system was competitive in either coordinate system; nonetheless, the existence proof given in this paper for a decreasing manifold only applies when the inequality (5.28) (or its alternative in (3.17)) applies. We also showed that when the Nagylaki–Crow model satisfies the inequalities (5.29), the invariant manifold is the graph of a convex function. In Fig. 4 we show that when (5.29) is not satisfied the invariant manifold, which still exists as two heteroclinic connections of axial and interior fixed points, may be non smooth and not the graph of a continuous decreasing convex function. How far the conditions for convexity can be weakened is an open problem.

Meanwhile, it is also unknown what conditions are required for the constructed invariant manifold to be smooth. Even when the model is competitive or strongly competitive, results such as in [19] are not immediately applicable as $\partial\mathbb{R}^2_+$ is not invariant for our system. Since f and g are bivariate polynomials each heteroclinic connection (orbit) along Σ is an analytic invariant manifold [20], hence only the interior fixed points on Σ need to be checked for C^1-smoothness. In addition, the Stable Manifold Theorem also indicates that the stable and unstable subspaces for any saddle point in the dynamical system are both one-dimensional. Moreover Σ, which is itself one-dimensional, must be tangential to one of the aforementioned subspaces, as well as C^1-smooth, even at the saddle point. Hence all that remains is to find conditions for Σ to be also C^1-smooth at interior fixed points of the model that are not saddles.

Recall that in Fig. 1 the invariant manifold Σ is not unique. In fact, numerics suggest that the model has a countable sequence of nonmonotone invariant manifolds; these are analogous to the family of manifolds described by Hirsch in Theorem 1.1 from [13]. Our model, however, is not immediately covered by Hirsch's results because the boundary of the phase space in Hirsch's system is invariant whereas in our case, the flow on the boundary points towards the interior of T. Nevertheless we believe that the difference is not problematic, as long as we have a repelling boundary for the phase space.

Appendix. The explicit equations for the Nagylaki–Crow model

This appendix explicitly provides the governing equations for the three genotype frequencies, and demonstrates that only two of the three equations are required.

By substituting (3.4) into Eq. (2.1), one has the following three equations of motion:

$$\begin{aligned}
\dot{x} &= \frac{1}{4}z^2F_{22} + x\left[y\left(D_3 - 2zF_{23}\right) + z\left(F_{12} + D_2\right) - y^2F_{33} - z^2F_{22} - D_1\right] \\
&\quad + x^2\left(-2yF_{13} - 2zF_{12} + F_{11} + D_1\right) - x^3F_{11} \\
\dot{y} &= \frac{1}{4}z^2F_{22} + y\left[x\left(D_1 - 2zF_{12}\right) + z\left(F_{23} + D_2\right) - x^2F_{11} - z^2F_{22} - D_3\right] \\
&\quad + y^2\left(-2xF_{13} - 2zF_{23} + F_{33} + D_3\right) - y^3F_{33} \\
\dot{z} &= 2xy\,F_{13} + z\left[y(F_{23} + D_3 - 2xF_{13}) + x(F_{12} + D_1) - x^2F_{11} - y^2F_{33} - D_2\right] \\
&\quad + z^2\left(-2yF_{23} - 2xF_{12} + \frac{1}{2}F_{22} + D_2\right) - z^3F_{22}.
\end{aligned}$$

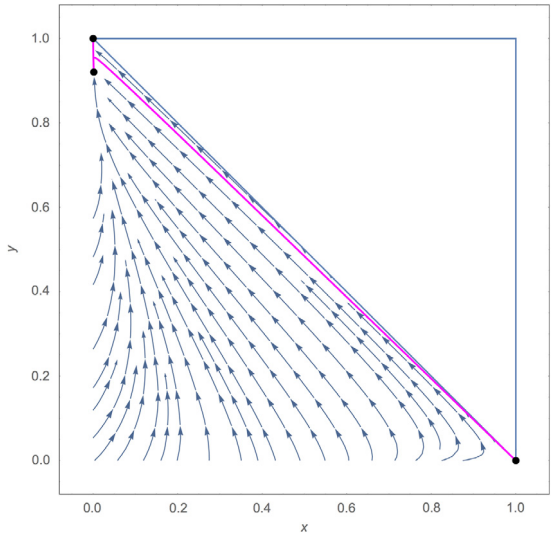

Fig. 4. A numerical example where the invariant manifold, which consists of a union of two heteroclinic orbits, is not nonmonotone, smooth or the graph of a convex function. The values of the fertilities are $F_{11} = 2/5$, $F_{12} = 1/100$, $F_{13} = 1/81$, $F_{22} = 98/100$, $F_{23} = 11/12$, $F_{33} = 1/97$, while the mortalities are $D_1 = 93/100$, $D_2 = 9/10$, $D_3 = 1/10$, so that this example does not satisfy either of $D_2 \leq D_1 + F_{23}$ or $D_2 \leq D_3 + F_{12}$.

But recall that $x + y + z = 1$. Due to this, one has $\dot{x} + \dot{y} + \dot{z} = 0$, rendering the z-equation redundant. Moreover, the remaining two equations can be re-written in terms of x and y:

$$\begin{aligned}
\dot{x} &= \frac{1}{4}y^2F_{22} - \frac{1}{2}yF_{22} + \frac{1}{4}F_{22} \\
&+ x\left(y\left(-F_{12} + \frac{5}{2}F_{22} - 2F_{23} - D_2 + D_3\right) + y^2(-F_{22} + 2F_{23} - F_{33})\right. \\
&\left.+F_{12} - \frac{3}{2}F_{22} - D_1 + D_2\right) \\
&+ x^2\left(y(2F_{12} - 2F_{22} + 2F_{23} - 2F_{13}) + F_{11} - 3F_{12} + \frac{9}{4}F_{22} + D_1 - D_2\right) \\
&+ x^3\left(-F_{11} + 2F_{12} - F_{22}\right) \\
\dot{y} &= \frac{1}{4}x^2F_{22} - \frac{1}{2}xF_{22} + \frac{1}{4}F_{22} \\
&+ y\left(x\left(-2F_{12} + \frac{5}{2}F_{22} - F_{23} + D_1 - D_2\right) + x^2(-F_{11} + 2F_{12} - F_{22})\right. \\
&\left.-\frac{3}{2}F_{22} + F_{23} + D_2 - D_3\right) \\
&+ y^2\left(x\left(2F_{12} - 2F_{22} + 2F_{23} - 2F_{13}\right) + \frac{9}{4}F_{22} - 3F_{23} + F_{33} - D_2 + D_3\right) \\
&+ y^3\left(-F_{22} + 2F_{23} - F_{33}\right).
\end{aligned}$$

References

[1] J. Hofbauer, K. Sigmund, Evolutionary Games and Population Dynamics, Cambridge University Press, Cambridge, 1998.
[2] L.S. Penrose, The meaning of "Fitness" in human populations, Ann. Eugenics 14 (4) (1949) 301–304.
[3] W.F. Bodmer, Differential fertility in population genetics models, Genetics 51 (3) (1965) 411–424.

[4] D.L. Rucknagel, J.V. Neel, The hemoglobinopathies, Prog. Med. Genet. (1961) 158–260.
[5] T. Nagylaki, J.F. Crow, Continuous selective models, Theoret. Popul. Biol. 5 (1974) 257–283.
[6] T. Nagylaki, Introduction to Theoretical Population Genetics, Springer-Verlag, Berlin, 1992.
[7] K.P. Hadeler, U. Liberman, Selection models with fertility differences, J. Math. Biol. 2 (1) (1975) 19–32.
[8] G.J. Butler, H.I. Freedman, P. Waltman, Global dynamics of a selection model for the growth of a population with genotypic fertility differences, J. Math. Biol. 14 (1) (1982) 25–35.
[9] K.P. Hadeler, D. Glas, Quasimonotone systems and convergence to equilibrium in a population genetic model, J. Math. Anal. Appl. 95 (2) (1983) 297–303.
[10] M. Koth, F. Kemler, A one locus-two allele selection model admitting stable limit cycles, J. Theoret. Biol. 122 (3) (1986) 263–267.
[11] J.M. Szucs, Equilibria and dynamics of selection at a diallelic autosomal locus in the Nagylaki-Crow continuous model of a monoecious population with random mating, J. Math. Biol. 31 (4) (1993) 317–349.
[12] E. Akin, J.M. Szucs, Approaches to the Hardy-Weinberg manifold, J. Math. Biol. 32 (7) (1994) 633–643.
[13] M.W. Hirsch, Systems of differential equations which are competitive or cooperative: III. Competing species, Nonlinearity 1 (1) (1988) 51–71.
[14] S. Boyd, L. Vandenberghe, Convex Optimization, Cambridge university press, 2004.
[15] S.A. Baigent, Convexity-preserving flows of totally competitive planar Lotka–Volterra equations and the geometry of the carrying simplex, Proc. Edinburgh Math. Soc. 55 (2012) 53–73.
[16] E.N. Dancer, P. Hess, Stability of fixed points for order-preserving discrete-time dynamical systems, J. Die Reine Angew. Math. 419 (1991) 125–139.
[17] J. Jiang, On the existence and uniqueness of connecting orbits for cooperative systems, Acta Math. Sin. New Ser. 8 (1986) 184–188.
[18] S.A. Baigent, Geometry of carrying simplices of 3-species competitive Lotka-Volterra systems, Nonlinearity 26 (4) (2013) 1001–1029.
[19] J. Mierczyński, Smoothness of unordered curves in two-dimensional strongly competitive systems, Appl. Math. 25 (4) (1999) 449–455.
[20] L. Perko, Differential Equations and Dynamical Systems, third ed., Springer-Verlag, New York, 2001.